

Evaluation Of A 4.5-kW D-100 Thruster With Anode Layer

Charles E. Garner*
Jet Propulsion Laboratory
California Institute of Technology
Pasadena, Ca 91109

S.O. Tverdokhlebov*, A. V. Semenkin, and V.I. Garkusha
Central Research Institute for Machine Building
Kaliningrad (Moscow Region), Russia

ABSTRACT

Design characteristics and performance data of a 4.5-kW, thruster with anode layer (TAL) developed at the Central Research Institute for Machine Building (TsNIMASH) are presented. The TAL is designated the D-1 (K) with a discharge chamber of outer diameter approximately 100 mm. Thruster performance was measured at TsNIMASH using a 1-ab6 hollow cathode and at JPL using a NASA-type BaO impregnated hollow cathode. Plume and performance characteristics were obtained over an input voltage range of 2.50-6(K) V and an input power range of 1.3 S-7.5 kW. Thruster efficiency increased with increasing discharge voltage and discharge current, and ranged from 0.42 at 300 V and 4.4 A up to over 0.62 at 600 V and 1 2.5 A. Plume divergence angle decreased with increasing discharge voltage and decreasing discharge current. The D-100 plume divergence angle at 1.34 kW is similar to the plume divergence angle measured for the SPT-100. At higher power levels the D-100 plume divergence angle is less than approximately 12 degrees, which implies that high-power TAL may be qualified with acceptable plume impacts on spacecraft systems such as solar arrays. Current and voltage oscillations are similar to those obtained in previous testing of an SPT-100 and a D-55 TAL. Performance characteristics demonstrated by the D-100 and life estimates by TsNIMASH make this thruster an excellent candidate for a wide range of station keeping, orbit raising, orbit maneuvering and Jovian planetary missions.

-r Group Leader, Advanced Propulsion Technology group

* Executive Director, TsNIMASH/Export, Kaliningrad, Russia

INTRODUCTION

In 1991 the innovative Science and Technology Office of the Ballistic Missile Defense Organization (BMDO) instigated a program to evaluate Hall thruster technology developed in the former Soviet Union [1]. Since that initial visit BMDO has pioneered the introduction of this technology to the west through a variety of programs and activities that include support of Space Systems/Loral's SPT-100 qualification program [2-6] and development of a prototype Hall thruster electric propulsion system called RHEET-1 (Russian Hall Effect Thruster Technology) [7]. BMDO's objective is to develop new electric propulsion technology and support commercialization of that technology through technology development programs and flight projects.

The thruster with anode layer (TAL) is one of the technologies identified in BMDO's ongoing Hall thruster evaluation program. The promising operating characteristics of the TAL

prompted BMDO's interest in these thrusters. The D-55 TAL, for example, has performance characteristics comparable to stationary plasma thrusters [8,9] but the TAL discharge chamber is physically smaller than that of the SPT-100. In addition, the mass of material eroded from a D-55 TAL may be less compared to the SPT-100 [9,10].

The physical principle of operation of the TAL was first proposed by A.V. Zharinov almost 30 years ago [11-13]. Early development of the TAL concentrated on the double-stage thruster [14,15]. By the end of the 1960's a double-stage TAL using bismuth as the propellant had been operated at up to 100 kW with a specific impulse of 8,000 s and a total efficiency of close to 0.8 [15,16].

By the 1970's, however, thruster development had outpaced the availability of high power in space and the program was redirected to emphasize development of low and medium power thrusters operating on rare gases. Research efforts centered on the development of

tion efficiency, single-stage thruster that could be operated on xenon [17-20].

The BMDO program has focused on thrusters that operate at an input power of 1.5 kW. However, thrusters that operate at a nominal input power of 4.5 kW were of interest for the BMDO Topaz program. The BMDO program has included evaluation of a "J"-160 SP1 developed at the Keldysh Research Institute for Thermal Processes (NIITP) [21] and a D-100 TAL developed at TsNIIMASH. The T-160 was evaluated at NIITP and NASA's Lewis Research Center (LARC) [22], and the D-100 TAL was developed at TsNIIMASH and evaluated at TsNIIMASH and JPL.

The D-1(K) TAL is a new, single-stage, high-power thruster designed to operate at a nominal input power of 300-15 A. It is different than its double-stage predecessor developed earlier at TsNIIMASH [23], which was developed for high specific-impulse missions. The D-100 was developed to operate efficiently at discharge voltages below 600 V.

Mission studies indicate that substantial mass savings are possible using D-1(K) technology for primary propulsion for orbit maintenance, orbit raising and for JPL planetary missions. Power levels available on commercial communication satellites are increasing, so the satellite industry will look to technologies such as the D-100 and "J"-160 to enhance competitiveness. This paper presents the results of a preliminary evaluation of the D-1(X) TAL; performance and plume characteristics over a thruster input power range of 1.34-7.5 kW are presented.

D-100 DESIGN FEATURES

The D-100 TAL plasma thruster is shown in Fig. 1. This thruster was tested using the same hollow cathode, employed in the D-55 anode layer wear test reported in Ref 9. The thruster has a discharge chamber outer diameter of approximately 100 mm, measured across the inner diameter of the outer ring cover. The distance, measured diagonally from the outer magnetic coils to the center of the thruster is approximately 180 mm. Thruster length is approximately 120 mm. Mass of the laboratory model D-100 thruster without a cathode is 7.17 kg.

The D-100 consists of two main parts: a magnetic system that creates the desired magnetic

field configuration at the thruster channel, and an anode assembly located near the downstream face of the thruster that serves as the positive electrode and provides for uniform distribution of the xenon in the discharge chamber. The magnetic circuit consists of one center electromagnet and four external electromagnets located at each corner of the thruster body. The series-connected external coils and the center coil are powered separately by two independent power supplies; magnetic coil power consumption, including both the inner and outer coils, is less than 15 watts at the maximum thruster power operating level of 7.5 kW.

The magnetic circuit provides a magnetic flux density at the discharge region of up to 0.1 T. It is made from soft iron and is used as the structure for all other thruster components that are mounted to the magnetic circuit. To enable high power operation the magnetic poles were fabricated from a cobalt alloy with a high Curie point to increase the demagnetization temperature. Graphite ring covers are located adjacent to the magnetic pole pieces to protect the pole pieces from erosion due to accelerated ion bombardment. Graphite was selected because of its superior thermal and sputtering properties.

The anode assembly is a welded toroidal structure with a graphite propellant distributor; use of graphite for this component increases thruster operating temperature capability and enhances the radiative cooling of the anode due to graphite's high emissivity. A cylindrical metallic grid with a transparency of 50% shields the external side surfaces of the anode assembly from arcing to nearby thruster components and the thruster body.

The cathode neutralizer is mounted to the thruster body on one side. During testing at TsNIIMASH, the D-100 was operated using a laboratory LaB6 cathode; this cathode was not optimized for operation with the D-100. Testing of the D-1(K) at JPL was performed using the same NASA hollow cathode employed for the D-55 evaluation and wear test.

JPL APPARATUS

The evaluation at JPL was performed in a 3.1-m dia. x 5.1-m stainless steel vacuum chamber equipped with three, each, 1.2-m diameter helium cryopumps. The minimum no-load tank pressure was observed to be 1.33×10^{-6} Torr.

5 Pa (1×10^{-7} Torr). The rated pumping speed for the three pumps combined is 81,000 liters/s cm xenon, however the measured pump speed cm xenon for this facility is approximately 50,000 l/s.

The thruster was mounted near one end of the vacuum tank, directly facing a cryopump which is positioned at the other end of the vacuum tank. To protect the cryopump and minimize the amount of material sputtered back to the thruster, the facility was lined with graphite as described in Ref. 6.

Tank pressure was measured using two ion gauges. One gauge tube was mounted directly to the outer wall of vacuum tank; the other tube was mounted inside the vacuum tank, approximately 0.51 m above and 0.58 m behind the 11-100. This tube was calibrated cm xenon and nitrogen using a spinning rotor gauge that is traceable to NIST.

The propellant system for supplying xenon to the D-100 thruster was constructed from 0.64-cm-dia stainless-steel tubing that was scrubbed with acetone and alcohol before assembly. The xenon supply pressure was indicated by a capacitance manometer that was calibrated to an accuracy of $\pm 0.25\%$ at 249.94 kPa. Micrometer valves located inside the vacuum chamber were used to control the flow rates to the discharge chamber and cathode. The pressure in the propellant tubing was above atmospheric pressure up to the micrometer valves. This design is believed to prevent oxygen contamination and cathode poisoning because those parts of the propellant system that are below atmospheric pressure are located inside the vacuum chamber.

Thermal mass flow meters were used to measure the total and discharge propellant flow rates. The flow meters were calibrated on xenon using a bubble volumeter. Because the flow meters available were inaccurate at flow rates typically used by the hollow cathode, the cathode flow rate was calculated by subtracting the discharge flow from the total flow rate. The bubble volumeter data cm xenon were curve fit and the curve fit was incorporated into the D-1 (K) data acquisition and control program.

In this paper and in previously reported Hall thruster data from this facility [6,9] the volumetric flow rates based cm bubble volumeter

calibrations were converted to mass flow rate using the Ideal Gas Law to calculate the conversion factor from standard cubic centimeters per minute (sccm) to mg/s. This conversion factor is: 1 sccm = 0.09753 mg/s.

However, based cm conversions with the National Institute for Standards and Technology (NIST) [24] and cm calculations performed for the NSTAR ion engine [25] a more accurate conversion factor may be: 1 sccm = 0.09838 mg/s.

If the conversion factor used for the NSTAR program is correct, data presented for the D-100 and for other Hall thrusters would require a slight correction to the calculated thruster flow rates and to calculated thruster efficiency.

The 1-1(K) was mounted in an inverted pendulum style thrust stand of the type developed at NASA LeRC [26]; in this design, thrust is indicated by a linear voltage displacement transducer (LVDT). The thruster was mounted to the thrust stand but was electrically isolated from the thrust stand and facility ground. Thermocouples were attached to the thruster body anti to the cathode for temperature measurements. The thrust stand is surrounded by a water-cooled, air housing to minimize temperature effects cm the measured thrust. Thrust stand inclination was adjusted continuously by computer to improve the accuracy of the thrust measurement. Thrust stand calibrations were performed in-situ throughout the 11-100 evaluation using a set of weights. Repeatability of the calibrations were normally better than 0.5%.

Thrust is determined from the difference in the LVDT voltage with the thruster cm and off, anti multiplying the LVDT voltage difference by a factor determined from the dead-weight in-situ calibration. The most accurate way to determine the "thruster off" LVDT voltage is to measure the LVDT voltage within one second of the thruster being turned off; in this way thrust stand drift due to thermal or other effects should be eliminated. However, thrust measured using this procedure does not include the small thrust element due to expansion of hot xenon out of the thruster.

Total thrust for the 1-1(K) reported herein is the sum of the measured electrostatic thrust plus an estimate of thrust provided by the hot

xenon flowing through the thruster. The estimate for thrust due to expansion of hot xenon out of the thruster was calculated using the following formula:

$$F = M_d(8kT / \pi m)^{1/2}, \text{ where}$$

F = Thrust due to expansion of xenon out of the D-100 (Nt)

M_d = Discharge flow rate (Kg/s)

k = Boltzman's constant

T = D-100 body temperature (K)

m = Xenon mass (2.18×10^{-25} Kg)

Thruster efficiency reported herein includes cathode flow rate, discharge power, and magnetic circuits power unless otherwise noted. The discharge flow rate was corrected for backflow using a simple mathematical model that is based on the vacuum tank pressure and the discharge chamber area of the D-100. Area for backflow calculations was estimated by TsNIIMAS11 and is assumed to be the area between the thruster pole pieces, which is approximately 62 cm^2 [28].

TsNIIMASH estimates that most backflow atoms that enter the discharge chamber are ionized, and that ionization of xenon that backflows into the thruster occurs in regions of low potential [28]. Backflow neutrals ionized in the discharge chamber contribute linearly to an increase in discharge power but may contribute only a small increment to the total thrust. If thrust does not increase substantially due to backflow of facility neutrals into the thruster, the efficiency reported in this paper will be conservative.

The thruster was operated using laboratory power supplies for the discharge and cathode igniter. The discharge supply limit was 600 V and 16 A, respectively, therefore it was not possible to obtain thruster data at discharge voltages exceeding 600 V. A DC low voltage start supply across the igniter and cathode emitter was used to start the cathode. No output filtering across the thruster was used.

A PC based data acquisition (DAC) system was used to monitor the vacuum facility, and to measure and record thruster data. A total of 56 channels that included thrust, xenon mass flow rate, anode voltage and current, floating voltage, magnet current and voltage, tank pressure and various other facility components were monitored and recorded as a function of

time. The data were averaged in real time and the averaged values were displayed on a monitor screen and recorded on the computer hard disc every 3-60 seconds; higher data recording rates were used during the first 30 minutes and last 5 minutes of thruster operation to examine various thruster operating characteristics and to obtain more precise thrust measurements.

JPL TEST PROCEDURE JRE

The 11-1(K) discharge and cathode, were purged with xenon when the mechanical pumps were used to pump the vacuum tank from atmosphere to 50 mTorr. The thruster was turned on by energizing the discharge supply and magnetic coils, and then igniting the cathode. A photograph of the D-100 operating in the JPL facility is shown in Fig. 2.

Thruster start-up procedure was as follows: thruster discharge flow was set to a maximum of 10 mg/s and the cathode flow to 0.6 mg/sec. Cathode flow was set to approximately 0.6 mg/s. Discharge voltage was set to a maximum of 600 V on the discharge power supply, and cathode igniter voltage was preset to 20 V. The internal and external magnetic coil power supplies were set to between 0.8- 1.1 A. Computer data storage frequency was set to every three seconds. After the cathode was conditioned via the tip heater the igniter supply was turned on, which always resulted in cathode ignition and thruster start. Normally the magnetic coil current did not require any adjustments after the thruster was started,

"The thruster was operated for one hour at 300 V and 10 A to heat and outgas the thruster. This procedure is especially important because outgassing by the graphite ring covers can result in a high current arc between the ring covers and the anode, which could possibly result in damage to the ring covers. Following operation for one hour at 3 kW, thruster performance was mapped by varying the discharge voltage, discharge current and flow rate. All performance measurements presented in this paper were obtained after the thruster had operated for a minimum of 10 minutes. Flow rate and thrust stand calibrations were performed after approximately every 8 hours of thruster operation, Plume data were recorded using a probe rake described in Ref. 6.

TsNIIMASH "TEST FACILITY"

Preliminary testing of the D-100 thruster at TsNIIMASHI was performed in a 1m x 6-m stainless-steel vacuum chamber equipped with five each, 0.8-m diameter oil diffusion pumps operated without cold traps to increase the pumping speed. Tank pressure while the thruster was in operation was $2-4.5 \times 10^{-2}$ Pa (not corrected for xenon) for a mass flow rate range of 6-13.5 mg/s. Tank pressure was measured using ionization gauges.

The discharge power supply is a cent rollable three-phase rectifier with an LC filter to smooth output voltage oscillations to less than $\pm 6\%$. The discharge circuit included a ballast resistor to limit the discharge current in the event of arcing or shorts. Internal and external magnetic coils were energized with independent current controlled power supplies providing a constant output current. Voltage and current measurements were obtained using analog meters with a measurement error of less than $\pm 1\%$.

The propellant system included independent cathode and discharge supply lines that were manually controlled using fine leak valves. Thruster flow rates were measured using a constant volume technique corrected for gas temperature and atmospheric pressure [29].

The thrust stand is a null-balance type described in detail in Reference 29.

Results and Discussion

I. Thrust and Efficiency

in Fig. 3 is plotted thrust and efficiency (cathode flow rate was included in the efficiency calculation) as a function of discharge voltage for a discharge current of approximately 7.4 A. The thrust values shown in Fig. 3 include a cold gas flow component as discussed. Uncertainty in the efficiency is due primarily to thrust measurement uncertainty. These data indicate that thrust and efficiency increase with increasing discharge voltage.

Thrust, efficiency, and specific impulse are shown as a function of discharge current in Figs. 4-11. The data in these figures indicate that thrust and efficiency increase with increasing discharge current and discharge voltage. Efficiency ranges from a low of 0.42 at 300 V and 4.42 A discharge to a high of 0.62 at a discharge voltage of 600 V and a discharge

current of 12.5 A (thruster input power = 7.5 kW). Specific impulse ranges from a low of 1,460 s at 3(K) V, 4.42 A to a high of 2,770 s at 600 V and 12.5 A. It is believed that the performance of the D-100 at 600 V and 12.5 A is the highest reported efficiency observed in Hall thruster testing in the west. Higher values of efficiency may be possible, since the thruster was not tested at its maximum discharge power.

Discharge efficiency is shown in Figs. 12-17. The data in these figures indicate that discharge efficiency increases with increasing discharge current, voltage, and power. Discharge efficiency ranges from a low of 0.45 at 300 V and 4.42 A to a high of 0.644 at a discharge voltage of 600 V and a discharge current of 12.5 A (thruster input power = 7.5 kW).

Data measured at TsNIIMASHI are shown in Table 1. Generally, the flow rate for a fixed discharge current and voltage measured at TsNIIMASHI is less than the flow rate measured at JPL. This is due likely to differences in pumping systems and flow calibration techniques at JPL and TsNIIMASHI. For a fixed discharge voltage and current, there is good agreement between JPL and TsNIIMASHI for data obtained between 300-350 V; at higher discharge voltages the thrust measured at TsNIIMASHI is generally greater than the thrust measured at JPL. Again, it is likely that the differences are due to use of different facilities, use of a different cathode, and to use of different methods for measuring thrust.

II* Plume Characteristics

Plume data for the D-100 measured at JPL are shown in Figs. 18-21. The distance between the probe and the downstream face of the D-100 was approximately 114 cm, similar to the distance used in measurements of the SPT-100 plume [Ref. 6]. The probe was covered with plasma-spray-coated tungsten to reduce the secondary electron emission coefficient [Ref. 6].

in Fig. 18 plume current density for a discharge voltage of 300 V and various discharge currents is plotted as a function of angle wrt the thruster axis. The data indicate that, for a fixed discharge voltage, the peak current density increases with increasing discharge current. In addition, the data indicate that the plume full angle at half-maximum (FWHM) increases with increasing discharge current. For example, the

FWHM for the case where the discharge current is 4.42 A is approximately 15 degrees, whereas the FWHM for the case where the discharge current is 12.52 A is approximately 20 degrees. The plume divergence angle for the SPT-100 was determined from previous testing to be approximately 16 degrees [Refs. 6, 27]. It is significant that the D-100 plume divergence angle at 1.34 kW is similar to the SPT-100 FWHM.

In Fig. 19 plume current density for a discharge current of approximately 7.5 ± 0.3 A and discharge voltages ranging from 250-500 V is plotted as a function of angle wrt the thruster axis. The abscissa in this graph was expanded for better pictorial resolution of the data. The data indicate that, for a fixed discharge current, the peak current density increases with increasing discharge voltage. In addition, the data indicate that the plume FWHM decreases with increasing discharge voltage. For example, the plume full angle for a discharge voltage of 250 V, 300 V, 400 V, and 500 V are approximately 30.7, 14.1, 14.1, and 11.9 degrees respectively. Significantly, these data indicate that under certain conditions the plume divergence angle may be less than approximate 14 degrees.

The plume current density profiles also exhibit a doubly-peaked profile as shown in Fig. 20. Generally, the greater the discharge voltage the more pronounced was the doubly-peaked profile. For the case where the discharge current was 4.2 A and the discharge voltage was 300 V, and for the case where the discharge current was 7.79 A and the discharge voltage was 250 V, no doubly-peaked profiles were observed. These data imply that at higher discharge voltages a somewhat annular-shaped plume structure is maintained due to superior focussing of the ion plume. Doubly-peaked plume profiles were not observed in the SPT-100 wear test [Ref. 6].

Plume profiles for the D-100 operated at 1.33 kW and 4.7 kW are shown in Fig. 21. At 1.33 kW the plume has a similar current density to that observed in the SPT-100, but the divergence angle of the D-100 is perhaps slightly less than the divergence angle for the SPT-100. At an input power to the D-100 of 4.7 kW, the current density is 2.9 times the current density at 300 V and 4.42 A, and the plume divergence angle is approximately 14.9 degrees.

III. Discharge Current and Discharge Voltage Oscillations

Discharge current and discharge voltage oscillations were measured at the vacuum chamber feedthrough in the same manner as discussed in Ref. 6. A laboratory power supply with 100 μ F across the supply output, but without external filtering, was used for the D-100 discharge in these tests. Oscillation data are shown in Figs. 22-23 for an input power of 2.1 kW and 7.5 kW respectively. Oscillation frequencies were typically approximately 33 kHz, which is similar to those observed in other Hall thruster tests [Refs. 6]. Current oscillation amplitudes increased with discharge current but never exceeded approximately 6 A peak-peak.

III. Discharge Current and Discharge

There are no data concerning operating life of the D-100. Estimates for wear characteristics of the D-100 are based on data from wear testing of the D-55 operated at 1.35 kW [9] and on known physics for the D-100. TsNIIMASH estimates that the operating life of the D-100 at 600 V and 7.5 A, corresponding to a thruster input power of 7.5 kW, is greater than 5,000 hours [Ref. 28]. The estimate is based on the fact that in the D-1(K) at 7.5 kW the plasma ion density is comparable to the D-55 at 1.35 kW, and that due to the larger physical size of the D-100 the ring covers and protective magnetic pole piece covers can be made thicker than in the D-100 model tested.

CONCLUSIONS

AD-100 thruster with anode layer (TAI) was evaluated at JPL and TsNIIMASH. A barium-calcium-aluminate hollow cathode fabricated at JPL was used to provide electrons for the discharge and to neutralize the beam, while TsNIIMASH used a laboratory LB6 cathode. Neither cathode was optimized for operation with a xenon-fueled D-100 TAI. Thruster efficiency increased with increasing discharge voltage and current, to a maximum of 0.62 at 600 V and 12.4 A. Thruster efficiency at a discharge voltage of 300 V and discharge current of 4.4 A was a respectable 0.42, demonstrating that the D-100 can be operated efficiently over a wide range of input power (1.35 to 7.5 kW). The maximum specific impulse measured was an impressive 2770 s including mass flow for the cathode, which is the highest specific impulse yet measured in a Hall thruster operated in the west. Plume data indicate that the plume divergence angle for the D-100 is comparable to or less than the SPT-100. Plume divergence angle increased with increasing

discharge current and decreased with increasing discharge voltage. Discharge current and voltage oscillations were similar to oscillations observed in other Hall thruster testing. TsNIIMASII estimates that the operating life of the D-100 at 7.5 kW is greater than 5,000 hours; this estimate is based on comparing ion current densities in the D-55 and D-100 and allowing for the potential to increase protective ring cover and pole piece cover thicknesses in the D-100.

"The excellent performance and wide range of efficient operation, combined with its operational simplicity, good plume characteristics and high thrust density make the D-100 TAI a good candidate for a number of future high power propulsion applications, including commercial communication satellite stationkeeping, high thrust orbit transfer propulsion systems, and for JPL planetary missions.

ACKNOWLEDGMENTS

The authors thank Dr. John Brophy, Mr. Alison Owens and Mr. Robert Toomath, for their efforts in support of the testing at JPL. The authors gratefully acknowledge the support of Dr. Len Caveny, Innovative Science and Technology office of the Ballistic Missile Defense Organization.

The work described in this paper was performed in accordance with JPL Contract N 959627 between TsNIIMASII/Export and the Jet Propulsion laboratory, California Institute of Technology, and was sponsored by the Ballistic Defense Missile Organization/Innovative Science and Technology office, through an agreement with the National Aeronautics and Space Administration.

REFERENCES

1. Brophy, J.R. et al., "Performance of the Stationary Plasma Thruster: SPT-100", AJAA-92-3155, July 1992.
2. Dickens, J. et al., "Impact of Hall Thrusters on communication System Noise", AIAA-95-2929, July 1995.
3. Day, M. et al., "SPT-100 Subsystem Qualification Status", AIAA-95-2666, July 1995.
4. D.H. Manzella, "Stationary Plasma Thruster Plume Emissions", IEPC-93-097,

Proceedings of the 23rd international Electric Propulsion Conference, September 1993.

5. T. Randolph et al., "Far-Field Plume Contamination and Sputtering of the Stationary Plasma Thruster", AIAA-94-2855, July 1994.

6. Garner, C.E. et al., "A 5,730-Hr Cyclic Endurance Test of the SFJ-100", IEPC-95-179, Proceedings of the 24th international Electric Propulsion Conference, September 1995.

7. L.H. Caveny et al., "The BMDO Electric Propulsion Flight Readiness Program", IEPC-95-132, Proceedings of the 24th International Electric Propulsion Conference, September 1995.

8. J.M. Sankovic et al., "Operating Characteristics of the Russian D-55 Thruster With Anode Layer", AIAA-94-3011, June 1994.

9. Garner, C.E., "Experimental Evaluation of Russian Anode Layer Thrusters", AIAA-94-3010, June 1994.

10. Marrese, C. et al., "Analysis of Anode Layer Thruster Guard Ring Erosion", IEPC-95-196, Proceedings of the 24th International Electric Propulsion Conference, September 1995.

11. Zharinov, A.V. and Popov, Yu. S., "Acceleration of Plasma by a Closed Hall Current", Sov. Phys. Tech. Phys. 12, pp. 208-211, August 1967.

12. Yushmanov, E.E., "Radial Distribution on Potential in the Cylindrical Magnetic Trap for Ion Injection on the Magnetron Type", in *Plasma Physics and the Problem of Controllable Thermonuclear Reactions*, 4, pp. 235-257, Academy of Sciences of the USSR, Moscow, 1958.

13. Grishin, S.D. et al., "Accelerators with Closed Hall Current", *Plasma Accelerators*, L.A. Artsymovich, ed., Mashinostroenie, Moscow, 1973.

14. Grishin, S.D. et al., *Electric Thrusters*, Mashinostroenie, Moscow, 1975.

15. Yerofeyev, V.S. et al., "Two-Stage Acceleration of Ions in Layer with Closed Hall Currents", *Plasma Accelerators*, L.A.

Artsymovich, ed., pp. 54-61, Mashinostroenie, Moscow, 1973.

16. Grishin, S.D. et al., "Characteristics of Two-Stage Ion Accelerators with Anode Layer", *Journal of Applied Mathematics and Technical Physics*, No. 2, pp. 28-36, 1978.

17. Yerofeyev, V.S. and Lyapin, Ye. A., "Integral Characteristics of Ion Source of Hall Accelerator with Anode Layer", Abstracts for II All-Union Conference on Plasma Accelerators, pp. 134-135, Minsk, 1973.

18. Lyapin, Ye. A. and Semenkin, A. V., "State-of-the-Art in investigations of Anode layer Accelerators", in *Ion Injectors and Plasma Accelerators*, pp. 20-33, Energoizdat, Moscow, 1990.

19. Garkusha, V.I. et al., "*Plasma Accelerators and injectors with Anode Layers*", pp. 129-138, Nauka, Moscow, 1984.

20. Semenkin, A. V., "Investigation of Erosion in Anode Layer Thruster and Elaboration High life Design Scheme", IFWC-93-231, Proceedings of the 23rd international Electric propulsion Conference, September 1993.

21. Sankovic, J.M. et al., "Performance Evaluation of a 4.5 kW SPT Thruster", IIPC-95-30, Proceedings of the 24th international Electric Propulsion Conference, September 1995.

2. Petrosov, V.A. et al., "Investigation of a 4.5 kW High Efficiency Hall-Type T-160 Electric Thruster", IIPC-95-31, Proceedings of the 24th International Electric Propulsion Conference, September 1995.

23. Tverdokhlebov, S.O., "Study of Double Stage Anode Layer Thruster Using Inert Gases", IIPC-93-232, Proceedings of the 23rd International Electric Propulsion Conference, September 1993.

24. Personal communication, June 13, 1995, Michael Moldover, National Institute of Standards and Technology, Gaithersburg, Md.

25. NSTAR reference.

26. Haag, T.W. and Curran, F. M., "Arcjet Starting Reliability: A Multistart Test on Hydrogen/Nitrogen Mixtures," AIAA-87-1061, May 1987. (NASA TM-898867).

27. Manzella, D.], and Sankovic, J. M., "Hall Thruster Ion Beam Characterization", AIAA-95-2927, July 1995.

28. Personal communication to Sergey Tverdokhlebov, May 21, 1996.

29. Semenkin, A. V. et al., "TsNIIMASH Activities in Electric Propulsion", IIPC-95-213, Proceedings of the 24th international Electric Propulsion Conference, September 1995.

Fig 1

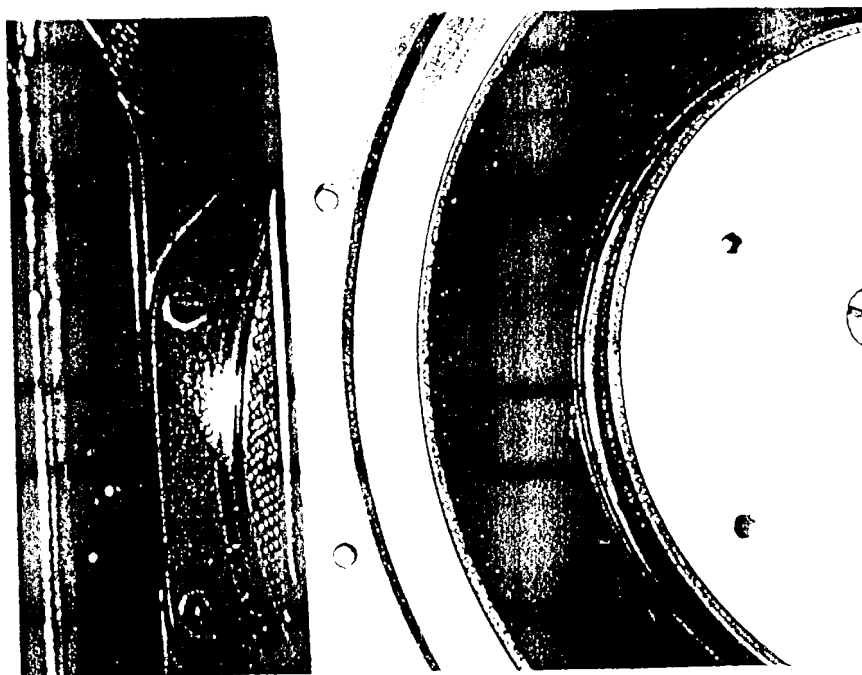
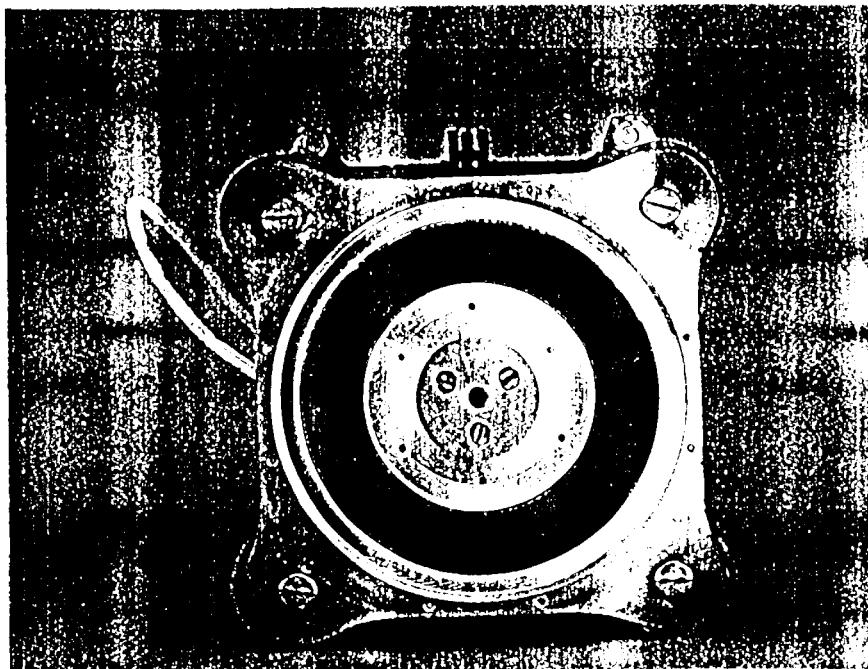


Fig 2

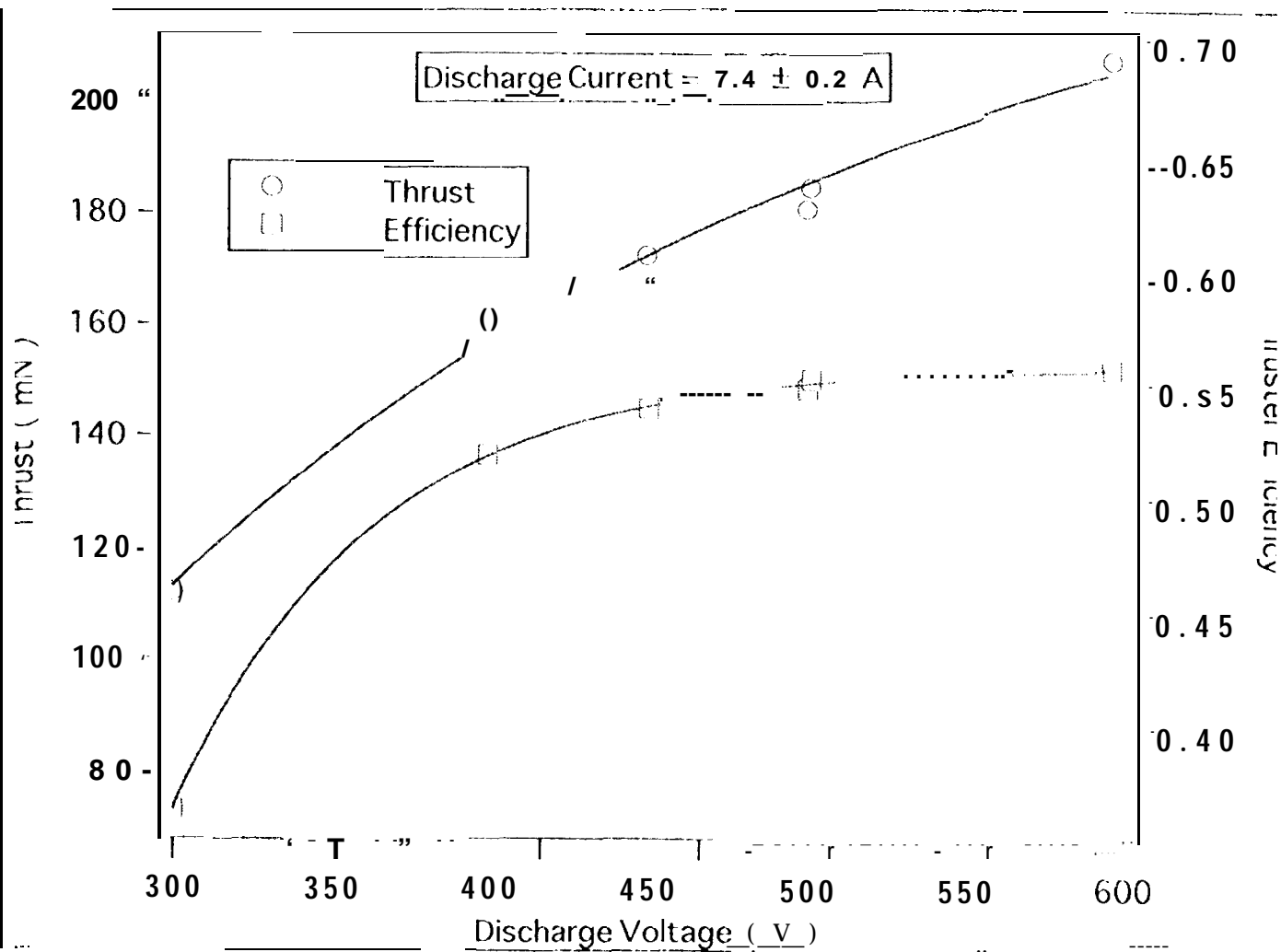


Fig. 3. Thrust and efficiency for a discharge current of 7.4 ± 0.2 A.

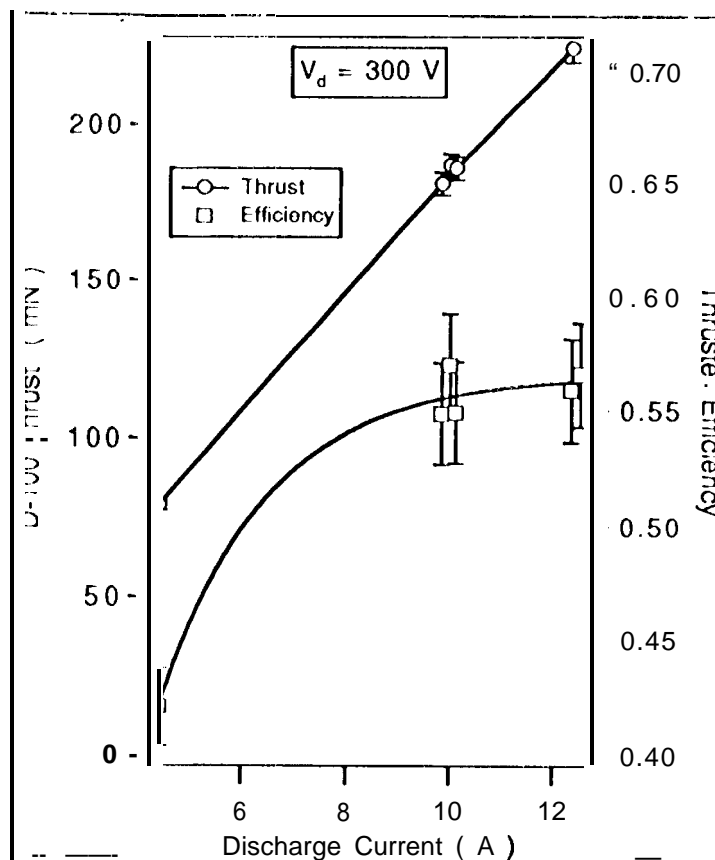


Fig. 4. Thrust and efficiency for a discharge voltage of 300 v.

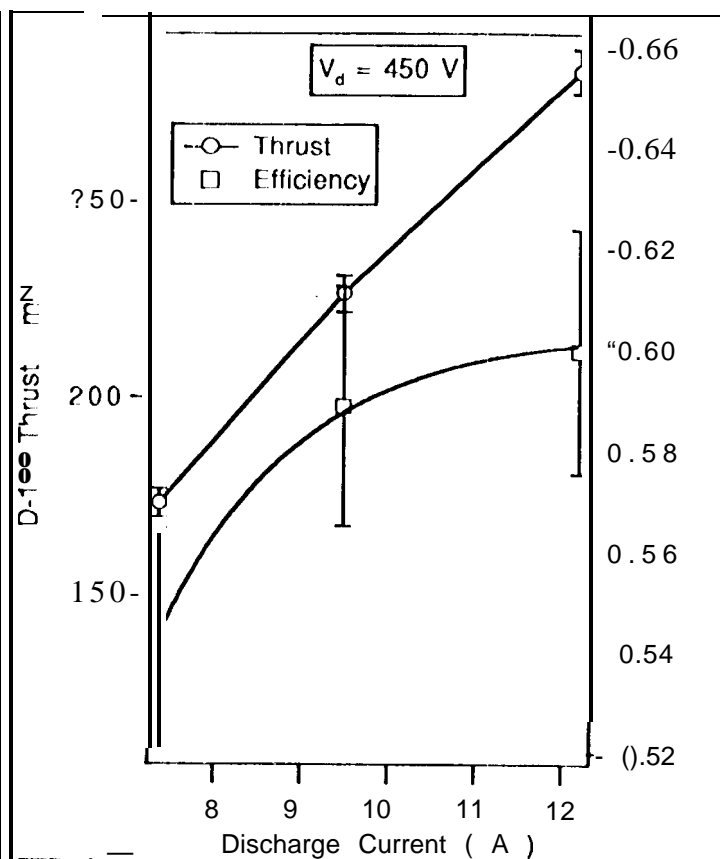


Fig. 5. Thrust and efficiency for a discharge voltage of 450 V.

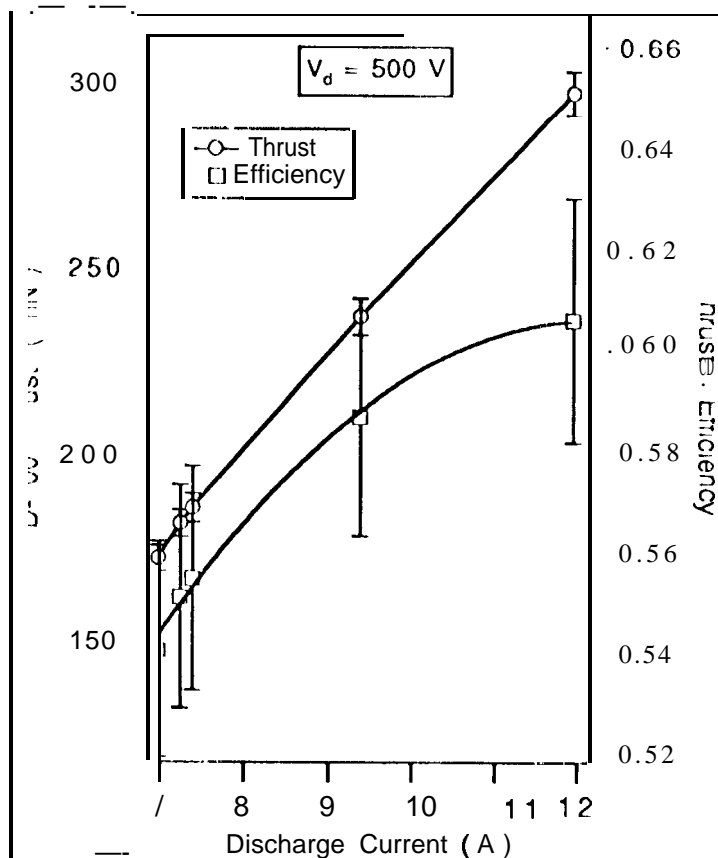


Fig. 6. Thrust and efficiency for a discharge voltage of 500 v.

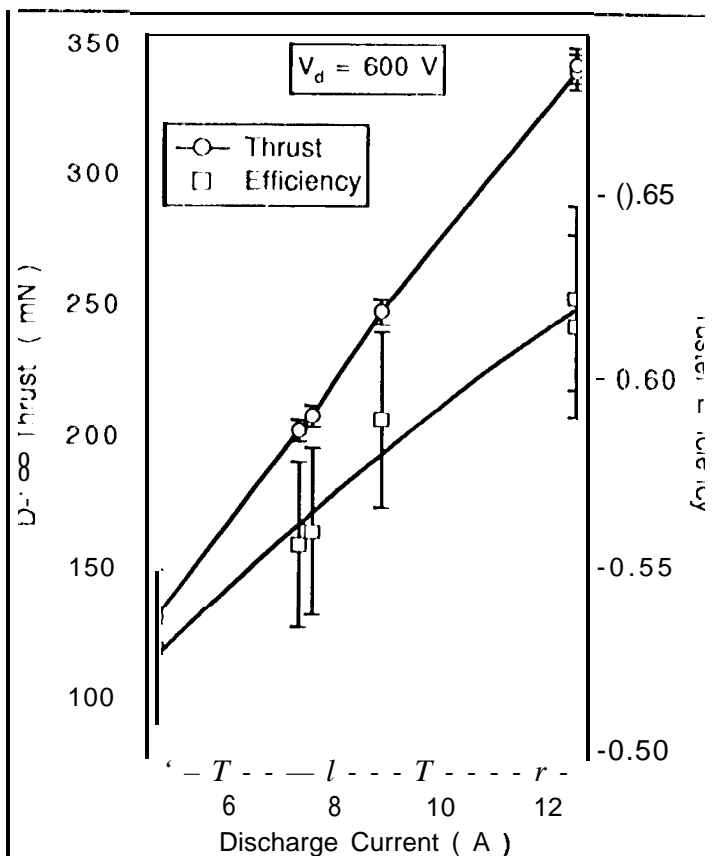


Fig. 7. Thrust and efficiency for a discharge voltage of 600 v.

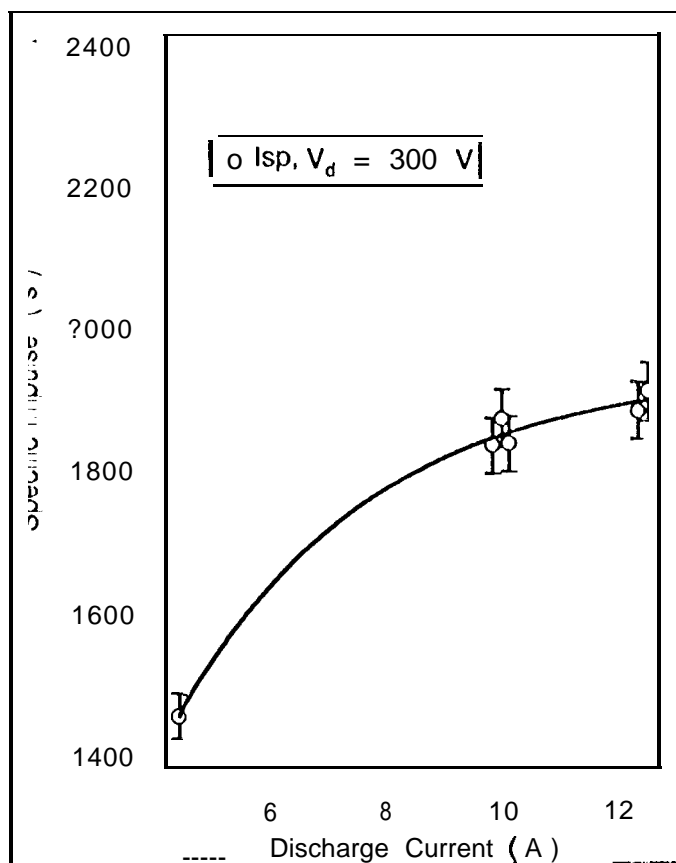


Fig. 8. Specific impulse for a discharge voltage of 300 v.

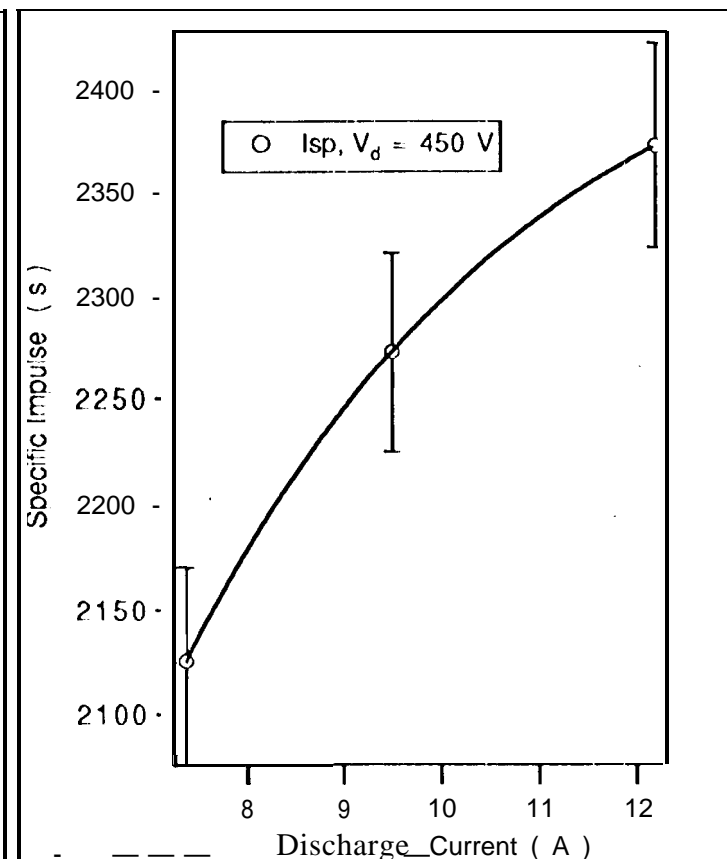


Fig. 9. Specific impulse for a discharge voltage of 450 v.

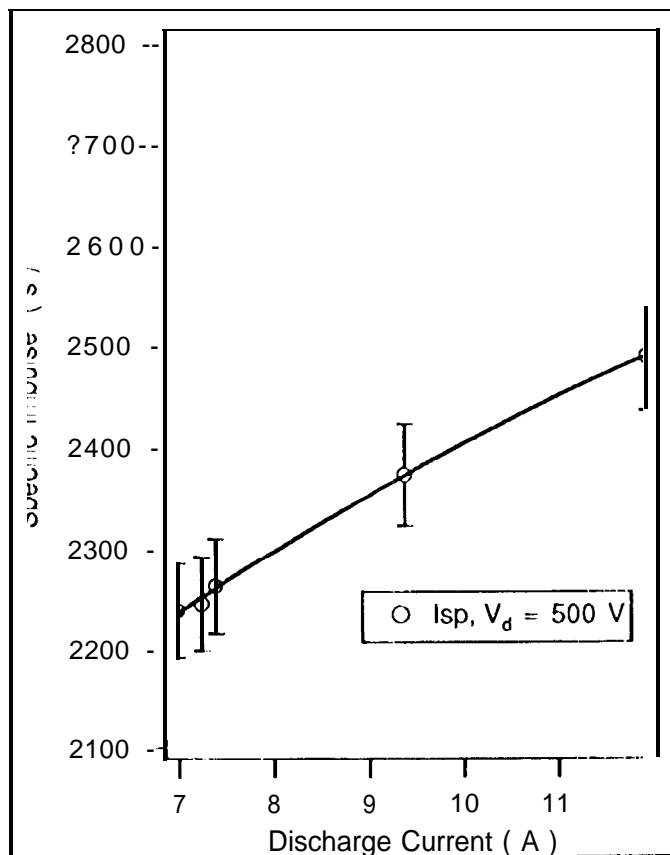


Fig. 10. Specific impulse for a discharge voltage of 500 v.

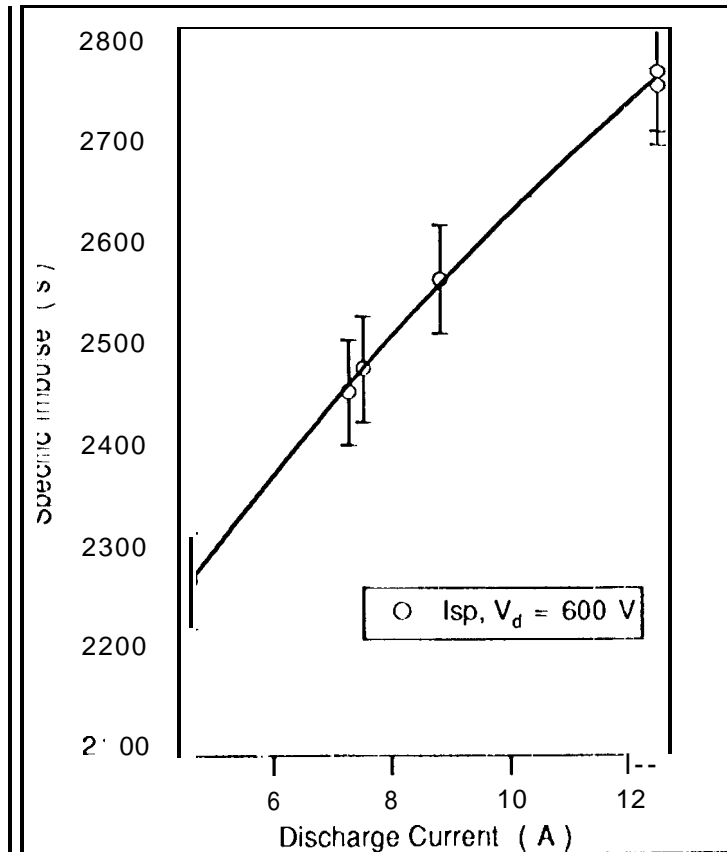


Fig. 11. Specific impulse for a discharge voltage of 600 V.

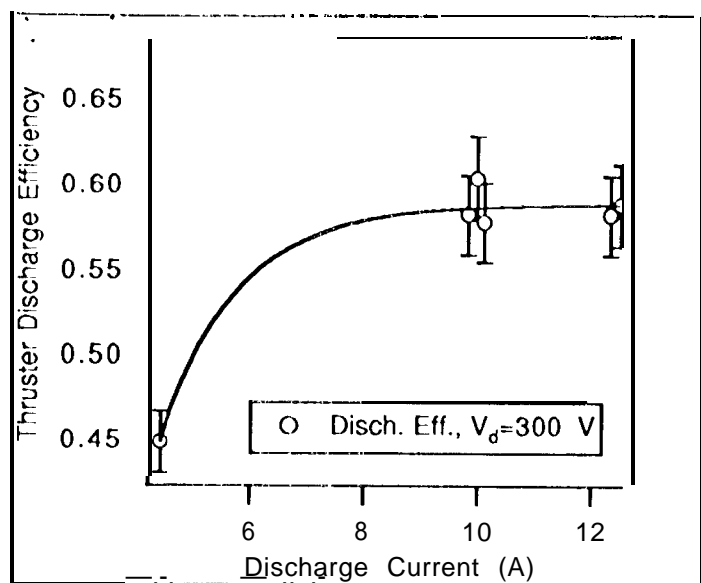


Fig. 12. Discharge efficiency for a discharge voltage of 300 V.

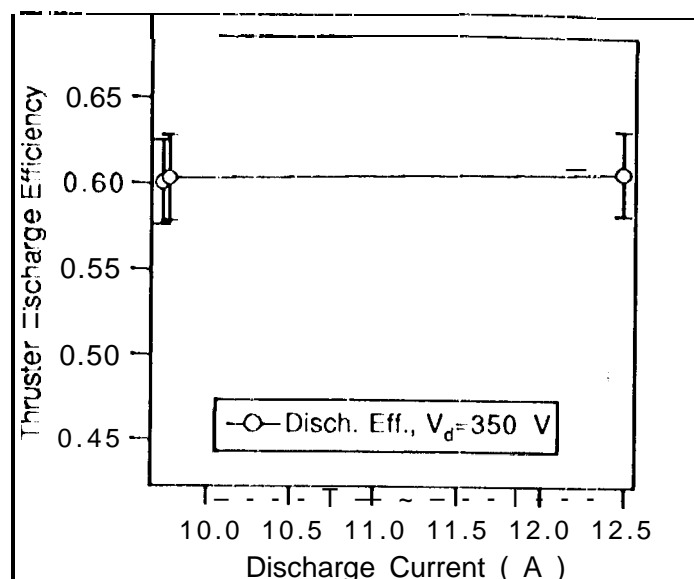


Fig. 13. Discharge efficiency for a discharge voltage of 350 v.

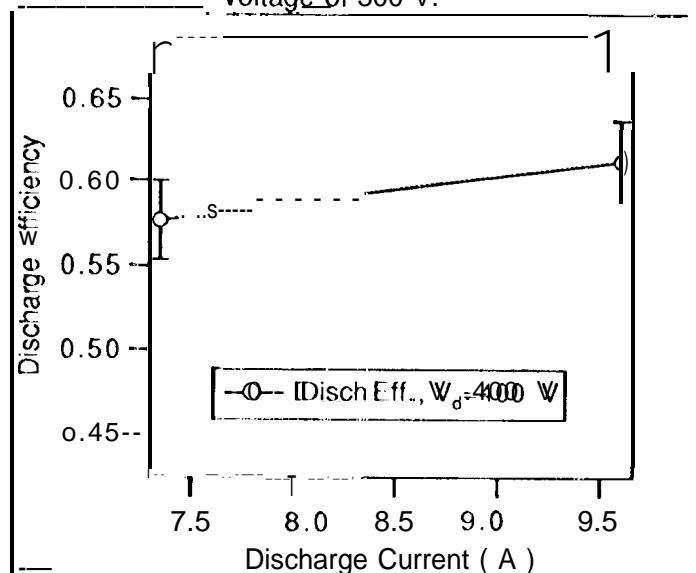


Fig. 14. Discharge efficiency for a discharge voltage of 400 V.

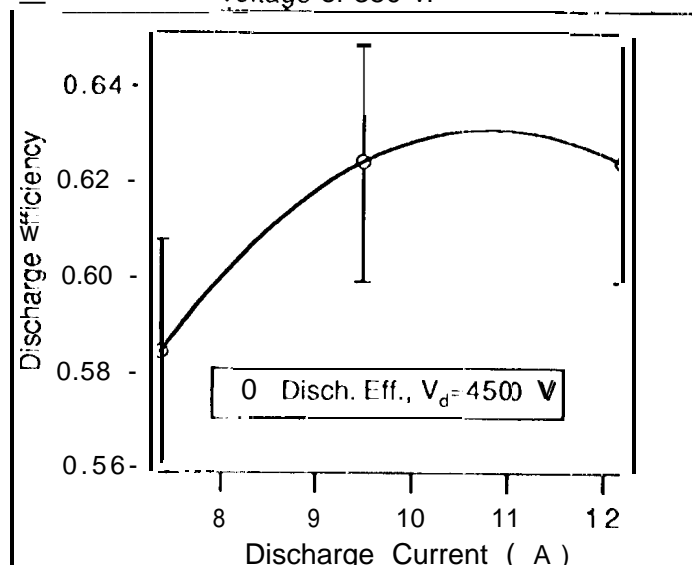


Fig. 15. Discharge efficiency for a discharge voltage of 450 V.

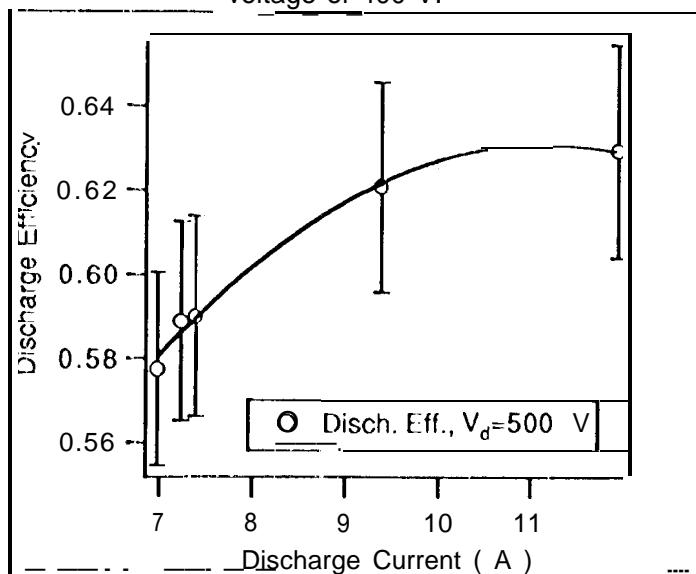


Fig. 16. Discharge efficiency for a discharge voltage of 500 V.

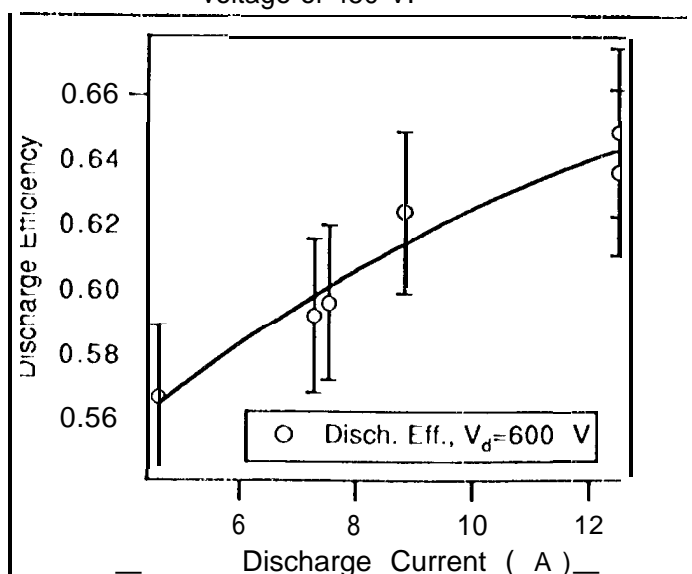


Fig. 17. Discharge efficiency for a discharge voltage of 600 V.

TABLE I

D-100 OPERATING CHARACTERISTICS MEASURED AT TsNIIMASH

Discharge Voltage v	Discharge Current A	Discharge Flow mg/s	Total Flow mg/s	Thrust g	specific Impulse s	Total* Thruster Efficiency
300	7.9	7.316	8.316	15.32	1842	57.16
300	10.0	9.208	10.208	19.14	1875	57.7
300	12.1	10.5	11.5	21.5	1869	53.6
300	14	12.42	13.42	24.84	1850.09	57.17
350	7.6	7.316	8.316	16.17	1944	56.7
350	9.7	9.208	10.208	20.2	1979	56.5
350	11.8	10.5	11.50	24.09	2094	58.6
350	15.9	13.76	14.76	30.70	2046	52.5
400	7.5	7.316	8.316	18.08	2174	62.9
400	9.5	9.208	10.208	22.36	2190	61.88
400	11.6	10.5	11.50	26.3	2286	62.2
400	15.5	13.76	14.76	33.8	2290	60.0
450	7.3	7.316	8.316	19.4	2302	63.7
450	9.3	9.208	10.208	23.87	2338	64.0
450	11.4	10.79	11.79	28.8	2442	61.7
450	14.4	12.93	13.93	33.94	2436	61.26
500	7.2	7.316	8.316	20.42	2455	66.8
500	9.2	9.208	10.208	25.38	2486	65.86
500	11.2	10.79	11.79	28.4	2408.8	58.6
500	13.2	13.7	14.7	35.10	2388	53.6

*includes cathode flow rate

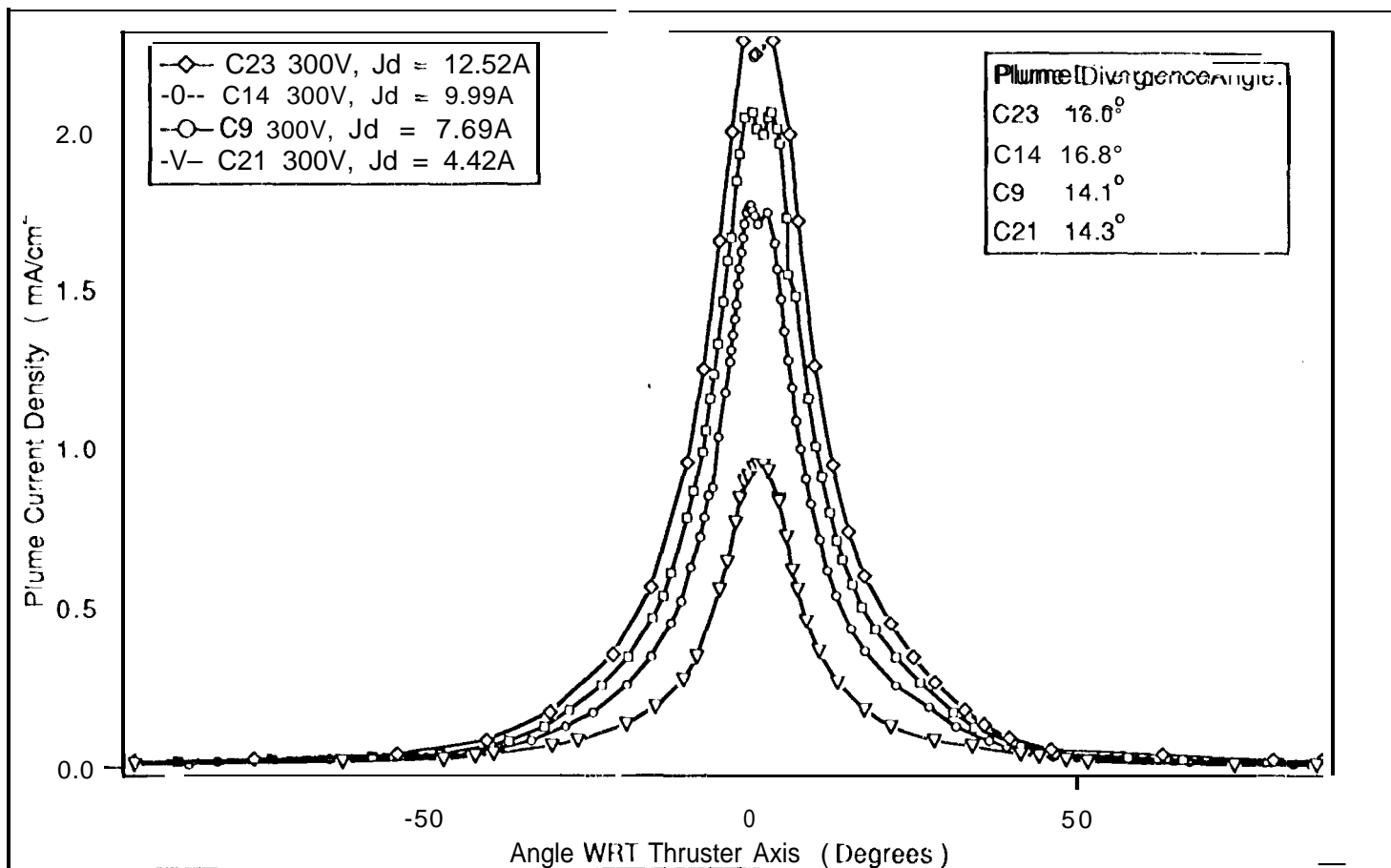


Fig. 18. Plume characteristics for a D-100 discharge voltage of 300 V.

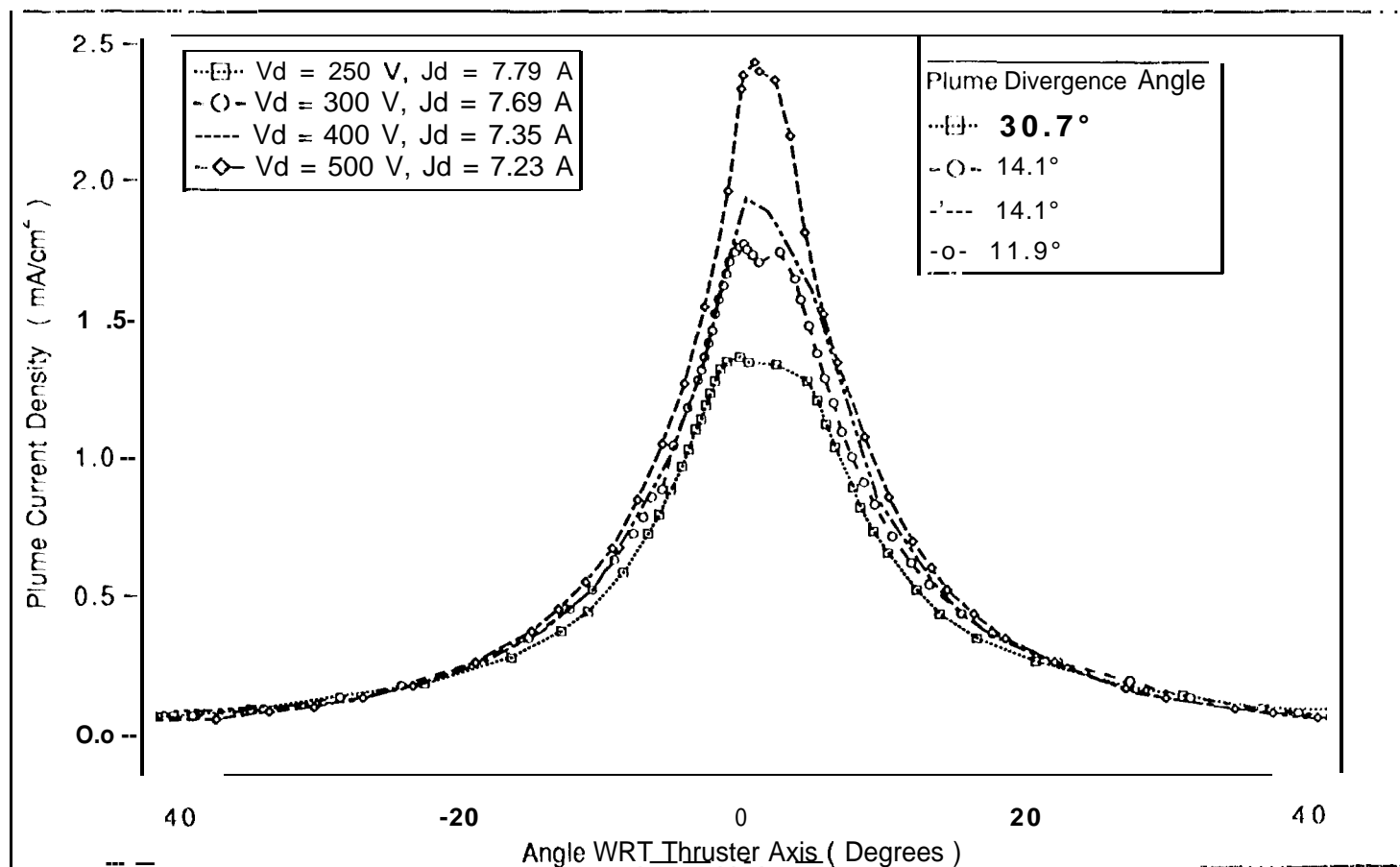


Fig. 19. Plume characteristics for a D-100 discharge current of 7.5:1 0.3 A.

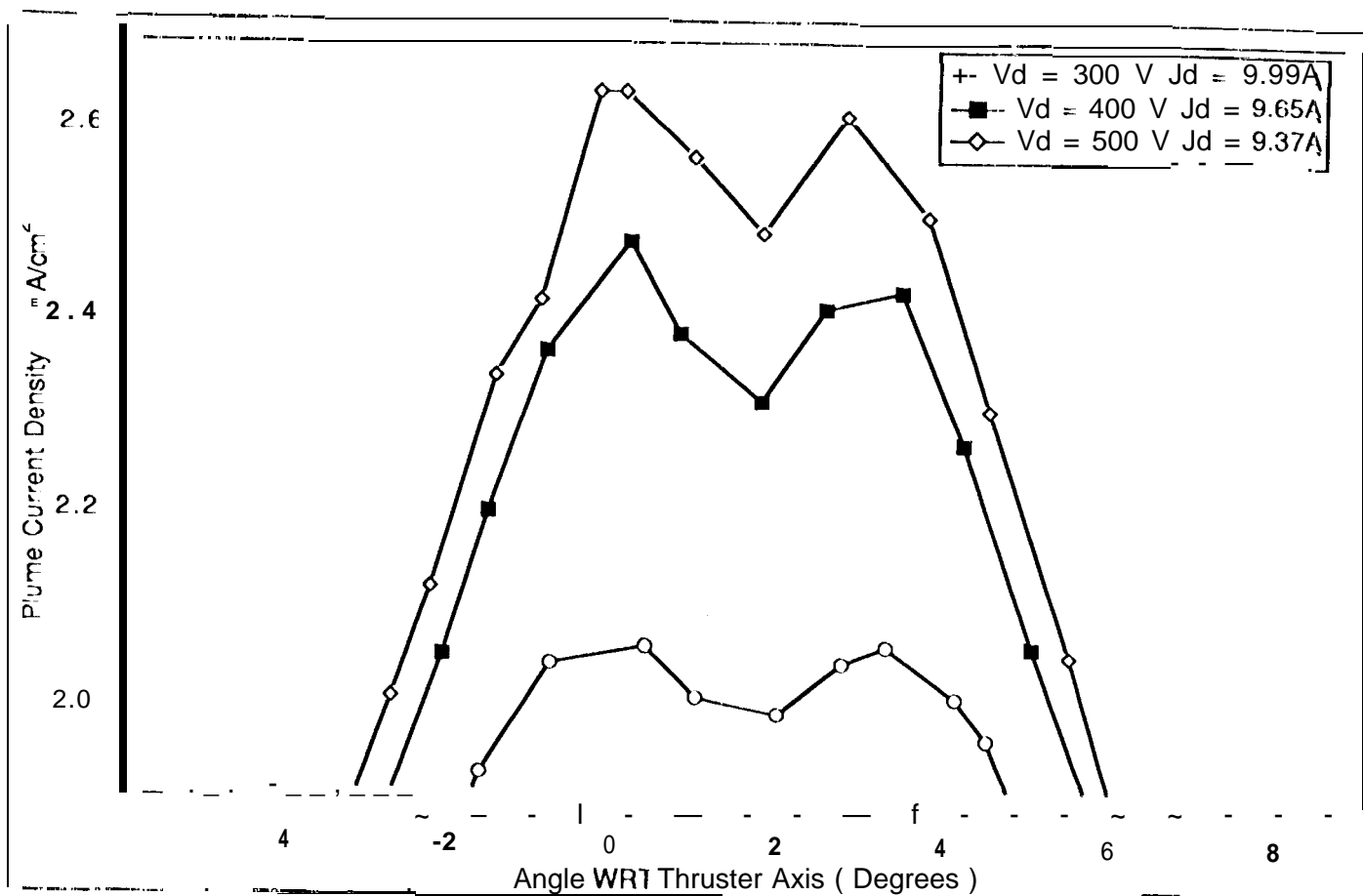


Fig. 20. Doubly-peaked plume profiles in the D-100 TAL.

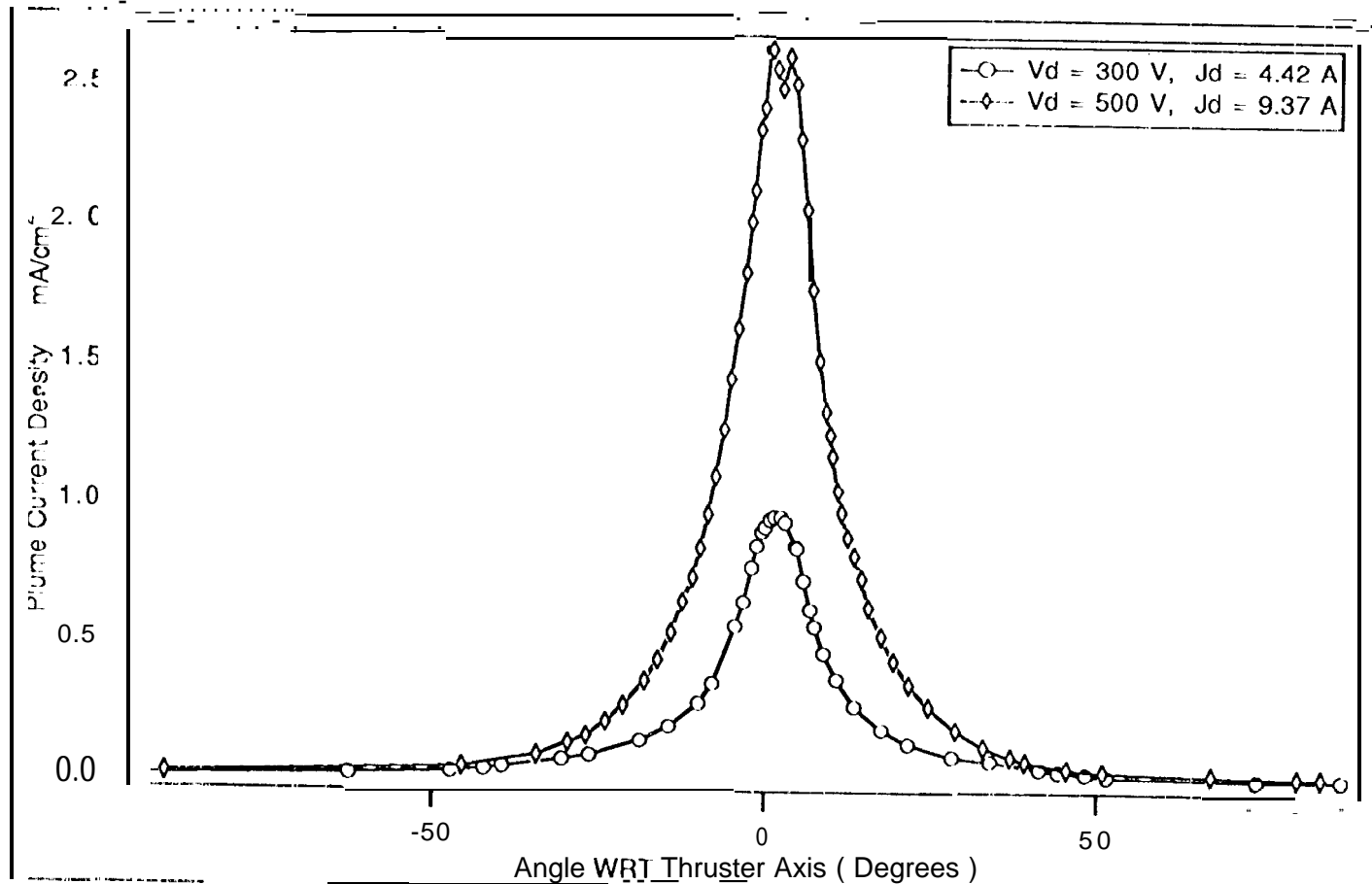
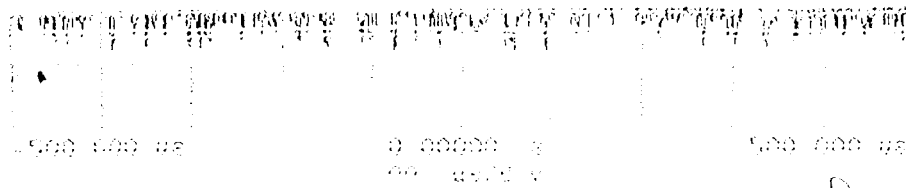


Fig. 21. Plume profiles for an input power to the D-100 TAL of 1.34 and 4.7 kW.



Should have
these retraced
by graphics

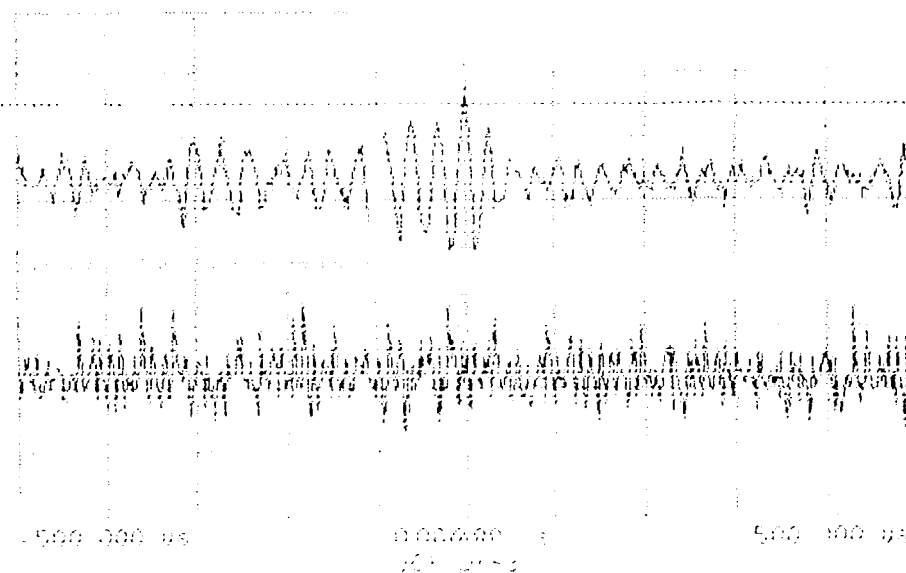
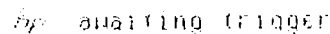
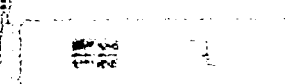
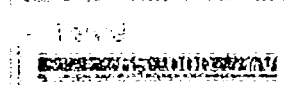
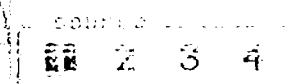
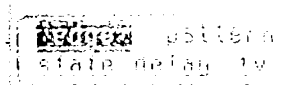
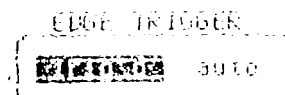
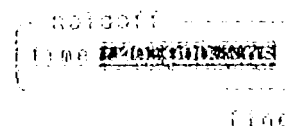


Fig 22-



021

299.8V

7.41 A

1A/div

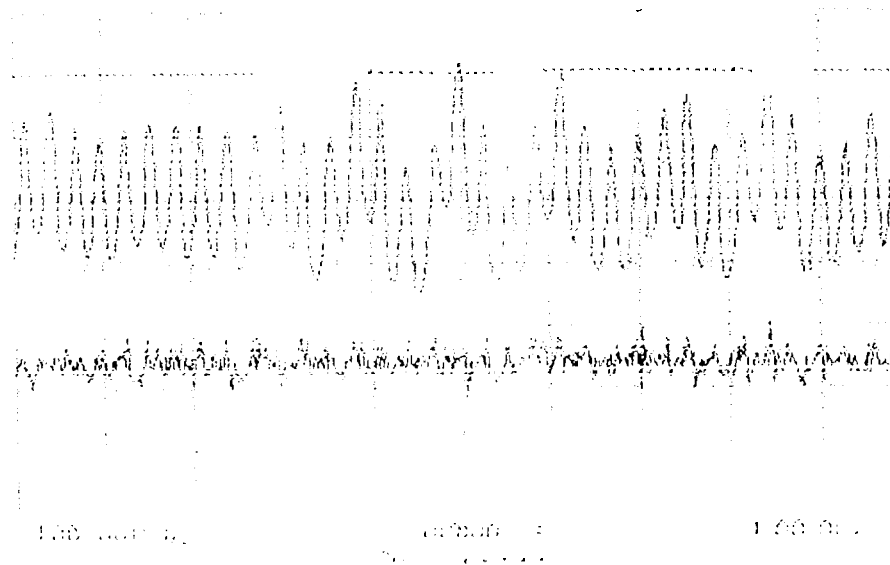
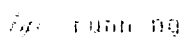
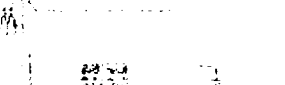
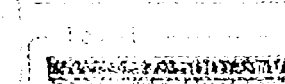
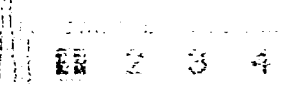
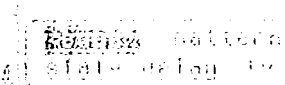
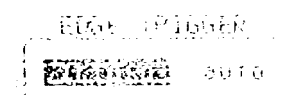
$$v/dv$$


Fig 23



047

2A lid

IV / dir

600V, 12.5